

**PREPARATION OF CHITOSAN DERIVATIVES
BY POLYETHYLENEIMINE MODIFICATION
FOR THE REMOVAL OF ACID RED 88 DYE**

NUUR HIDAYAH BINTI YUSOF

UNIVERSITI SAINS MALAYSIA

2019

**PREPARATION OF CHITOSAN DERIVATIVES
BY POLYETHYLENEIMINE MODIFICATION
FOR THE REMOVAL OF ACID RED 88 DYE**

by

NUUR HIDAYAH BINTI YUSOF

**Thesis submitted in fulfilment of the requirements
for the degree of
Master of Science**

August 2019

ACKNOWLEDGEMENT

First and foremost, I would like to express my sincere gratitude to my dear supervisor, Dr. Sumiyah Sabar, for her advice, critics, encouragement and patience throughout the course of this work. The present work has been financially supported by the Ministry of Education (MOE) under the Fundamental Research Grant Scheme (FRGS) (203/PJJAUH/6711445) and the Universiti Sains Malaysia (USM) under the Bridging Grant (304/PJJAUH/6316074).

My special appreciation also goes to my co-supervisor, Professor Dr. Bassim H. Hameed, Dr. Mohd Hazwan Hussin and Assoc. Prof. Dr. Foo Keng Yuen for their guidance and support. I am also indebted to all the laboratory personnel, particularly to Mr Azizo bin Daud, Mr Muhammad Ikhwan Harun, Mr Sivaraj a/l Panirselvam and Mr Yushamdan Yusof for their excellent and prompt service during FTIR, SEM, BET and XRD analysis, respectively. I would also like to thank my lab mates Ms. Caryn Tan, Mr Tan, Mrs Tina and Mrs Zahidah, for their sincere assistances and useful discussions. Not forgetting all the respective lecturers and staffs of School of Distance Education, School of Chemical Science and Institute of Postgraduate Studies (IPS) for the help given, either directly or indirectly.

Finally, I would like to express my boundless appreciation to my beloved parents, Mr Yusof Adon and Mrs Hamidah Junit for their never-ending love, support, understanding and patience throughout the duration of my study. May Allah S.W.T always give us all His blessings and ease out path in the future.

TABLE OF CONTENTS

Acknowledgement	ii
Table of contents	iii
List of tables	vii
List of figures	viii
List of abbreviations and symbols	x
Abstrak	xiii
Abstract	xv
CHAPTER 1 – INTRODUCTION	
1.1 Research background	1
1.2 Problem statements	4
1.3 Research objectives	5
1.4 Scope of study	6
CHAPTER 2 – LITERATURE REVIEW	
2.1 Adsorption	7
2.2 Adsorption isotherm	8
2.2.1 Langmuir isotherm model	10
2.2.2 Freundlich isotherm model	12
2.2.3 Temkin isotherm model	12
2.3 Adsorption kinetics	13
2.3.1 Pseudo-first-order model	14
2.3.2 Pseudo-second-order model	14
2.4 Diffusion-controlled sorption mechanism	15

2.5	Thermodynamics	16
2.6	Low cost adsorbents (LCAs)	17
2.7	Chitosan	18
2.7.1	Production of chitosan	18
2.7.2	Properties of chitosan	20
2.7.3	Applications of chitosan	22
2.8	Modification of chitosan	23
2.8.1	Physical modification	23
2.8.2	Chemical modification	24
	2.8.2(a) Graft copolymerization of chitosan	25
	2.8.2(b) Cross-linking of chitosan	29
2.8.3	Hydrothermal synthesis	31
2.9	Acid Red 88 (AR88) as a model pollutant	34
CHAPTER 3 - MATERIALS AND METHODS		
3.1	Chemicals and reagents	35
3.2	Instruments and equipment	35
3.3	Preparation of dye aqueous solution	36
3.4	Preparation of chitosan solution	36
3.5	Preparation of polyethyleneimine-grafted-cross-linked-chitosan	37
3.5.1	Effect of polyethyleneimine concentrations	37
3.5.2	Effect of cross-linker concentrations	38
3.5.3	Effect of heating temperatures	38
3.5.4	Effect of heating time	38
3.6	Characterization of adsorbents	39

3.6.1	Scanning electron microscope coupled with energy dispersive X-ray spectrometer (SEM-EDX)	39
3.6.2	Attenuated total reflectance Fourier transform infrared (ATR-FTIR) spectroscopy	39
3.6.3	X-ray diffraction (XRD) analysis	40
3.6.4	Surface area and porosity analysis	40
3.6.5	Determination of point of zero charge (pH_{pzc})	40
3.7	Batch adsorption studies	41
3.7.1	Effect of initial dye concentration and contact time	41
3.7.2	Effect of initial pH solution	42
3.8	Adsorption isotherms	42
3.9	Adsorption kinetics	42
3.10	Thermodynamics	43

CHAPTER 4 – RESULTS AND DISCUSSION

4.1	Preparation of polyethyleneimine-grafted-cross-linked-chitosan	44
4.1.1	Effect of polyethyleneimine concentrations	44
4.1.2	Effect of cross-linker concentrations	46
4.1.3	Effect of heating temperatures	47
4.1.4	Effect of heating time	49
4.2	Characterization of the adsorbents	50
4.2.1	Scanning electron microscope coupled with energy dispersive X-ray spectrometer (SEM-EDX)	51
4.2.2	Attenuated total reflectance Fourier transform infrared (ATR-FTIR) spectroscopy	54
4.2.3	X-ray diffraction (XRD) analysis	61

4.2.4	Surface area and porosity analysis	63
4.2.5	Determination of point of zero charge (pH_{pzc})	64
4.3	Batch adsorption studies	66
4.3.1	Control experiment	66
4.3.2	Effect of initial dye concentrations and contact time	68
4.3.3	Effect of initial pH solution	71
4.4	Adsorption isotherms	73
4.5	Adsorption kinetics	80
4.6	Diffusion models	83
4.6.1	Intra-particle diffusion	83
4.6.2	Boyd model	87
4.7	Thermodynamics	90

CHAPTER 5 – CONCLUDING REMARKS AND SUGGESTIONS FOR FUTURE STUDIES

5.1	Conclusions	92
5.2	Suggestions for future studies	94

REFERENCES	95
-------------------	-----------

APPENDICES

LIST OF PUBLICATIONS, CONFERENCES AND EXHIBITIONS

LIST OF TABLES

	Page
Table 1.1 Typical dyes used in the textile industry (Salleh <i>et al.</i> , 2011).	2
Table 2.1 Characteristics of physisorption and chemisorption (Konicki <i>et al.</i> , 2013).	7
Table 2.2 Chitosan properties in relation to the water and waste treatment applications (Renault <i>et al.</i> , 2009).	22
Table 2.3 Summary of studies on graft copolymerization of chitosan with various monomers using different techniques.	26
Table 2.4 Cross-linkers commonly used and their properties (Józwiak <i>et al.</i> , 2017).	29
Table 2.5 Summary of related work on modification of chitosan under hydrothermal treatment and their applications in different fields.	33
Table 4.1 Elemental composition of Cs, CsPC, CsPE and CsPG.	53
Table 4.2 Textural properties of Cs, CsPC, CsPE and CsPG.	63
Table 4.3 Isotherm adsorption parameters for the adsorptive uptake of AR88 onto CsPC, CsPE and CsPG at 30 °C.	76
Table 4.4 Comparison of the maximum adsorption capacities, q_m of AR88 onto various adsorbents.	78
Table 4.5 Adsorption kinetic parameters for the adsorptive uptake of AR88 onto CsPC, CsPE and CsPG at different initial dye concentrations.	82
Table 4.6 Intra-particle diffusion model parameters for the adsorptive uptake of AR88 onto CsPC, CsPE and CsPG at different initial dye concentrations.	84
Table 4.7 Film diffusion model parameters for the adsorption of AR88 onto CsPC, CsPE and CsPG at different initial dye concentrations.	89
Table 4.8 Thermodynamic parameters for the adsorption of AR88 onto CsPC, CsPE and CsPG at 30, 40 and 50 °C.	91

LIST OF FIGURES

		Page
Figure 1.1	Percentages attributed by different industries on water contamination by dyes (Katheresan <i>et al.</i> , 2018).	1
Figure 2.1	System of isotherm classification for solid solute adsorption (SSA) (Giles <i>et al.</i> , 1974).	9
Figure 2.2	Structure of (a) chitin and (b) partially deacetylate chitosan (Zohuriaan-mehr, 2005).	19
Figure 2.3	Molecular structure of Acid Red 88 (AR88) (Akar <i>et al.</i> , 2013).	34
Figure 4.1	The effect of PEI concentrations on the amount of AR88 uptake by CsPC, CsPE and CsPC with initial dye concentration of 100 mg L ⁻¹ , temperature of 30 °C and contact time of 24 h.	45
Figure 4.2	The effect of cross-linker concentrations on the amount of AR88 uptake by CsPC, CsPE and CsPG with initial dye concentration of 100 mg L ⁻¹ , temperature of 30 °C and contact time of 24 h.	46
Figure 4.3	Effect of heating temperatures on the amount of AR88 uptake by CsPC, CsPE and CsPG with initial dye concentration of 100 mg L ⁻¹ , temperature of 30 °C and contact time of 24 h.	48
Figure 4.4	Effect of heating time on the amount of AR88 uptake by CsPC, CsPE and CsPG with initial dye concentration of 100 mg L ⁻¹ , temperature of 30 °C and contact time of 24 h.	50
Figure 4.5	SEM image of Cs at 6,000 × magnification.	51
Figure 4.6	SEM images of CsPC a) before, and b) after AR88 adsorption; CsPE c) before and d) after AR88 adsorption; CsPG e) before and f) after AR88 adsorption at 6,000× magnification.	52
Figure 4.7	FTIR spectra of Cs, PEI and CsPC before and after AR88 adsorption	55
Figure 4.8	Proposed molecular structure of CsPC (Mahaninia and Wilson, 2016).	56
Figure 4.9	Proposed molecular structure of CsPE (Chatterjee <i>et al.</i> , 2011).	57
Figure 4.10	FTIR spectra of CsPE before and after AR88 adsorption.	58

Figure 4.11	Proposed molecular structure of CsPG (Chassary <i>et al.</i> , 2005).	59
Figure 4.12	FTIR spectra of CsPG before and after AR88 adsorption.	60
Figure 4.13	XRD pattern of Cs, CsPC, CsPE and CsPG.	62
Figure 4.14	pH point of zero charge (pH_{pzc}) of (a) CsPC, (b) CsPE and (c) CsPG.	65
Figure 4.15	Control experiment for the adsorption of AR88 by Cs, CsC, CsE, CsG, CsPC, CsPE and CsPG at initial dye concentration of 100 mg L^{-1} , temperature of $30 \text{ }^\circ\text{C}$ and contact time of 24 h.	67
Figure 4.16	The effect of initial dye concentrations and contact time on the amount of AR88 adsorbed by (a) CsPC, (b) CsPE, and (c) CsPG at temperature of $30 \text{ }^\circ\text{C}$ and contact time of 24 h.	68
Figure 4.17	The effect of initial pH on the adsorption of AR88 by CsPC, CsPE and CsPG with initial dye concentration of 100 mg L^{-1} , temperature of $30 \text{ }^\circ\text{C}$ and contact time of 24 h.	71
Figure 4.18	Adsorption equilibrium on the adsorption of AR88 by CsPC, CsPE and CsPG at different dye concentrations at temperature of $30 \text{ }^\circ\text{C}$ and contact time of 24 h.	74
Figure 4.19	Linear plots of the Langmuir isotherm model for the adsorptive uptake of the AR88 onto CsPC, CsPE and CsPG at different initial dye concentrations at $30 \text{ }^\circ\text{C}$.	75
Figure 4.20	Linear plots of the Freundlich isotherm model for the adsorptive uptake of the AR88 onto CsPC, CsPE and CsPG at different initial dye concentrations at $30 \text{ }^\circ\text{C}$.	79
Figure 4.21	Linear plots of the Temkin isotherm model for the adsorptive uptake of the AR88 onto CsPC, CsPE and CsPG at different initial dye concentrations at $30 \text{ }^\circ\text{C}$.	80
Figure 4.22	Intra-particle diffusion model plots for the adsorption of AR88 by a) CsPC, b) CsPE and c) CsPG at different initial dye concentrations, temperature of $30 \text{ }^\circ\text{C}$ in 24 h.	85
Figure 4.23	The Boyd diffusion model plots for the adsorption of AR88 by a) CsPG, b) CsPE and c) CsPG at different initial dye concentrations, temperature of $30 \text{ }^\circ\text{C}$ in 24 h.	87
Figure 4.24	Van't Hoff plot for the adsorption of AR88 by CsPC, CsPE and CsPG at initial dye concentration of 100 mg L^{-1} and contact time 24 h.	90

LIST OF ABBREVIATIONS AND SYMBOLS

AR88	Acid Red 88
E_a	Activation energy (kJ mol^{-1})
n	Adsorption intensity of the adsorption process
q_t	Amounts of dye adsorbed on the adsorbent at time, t (mg g^{-1})
ATR	Attenuated total reflectance
A	Binding constant at equilibrium (L g^{-1})
C	Boundary layer thickness (mg g^{-1})
BET	Brunauer-Emmett-Teller
$q_{e, cal}$	Calculated adsorption capacity of the adsorbent (mg g^{-1})
Cs	Chitosan
C_{Ad}	Concentrations of the adsorbate adsorbed on solid at equilibrium (mg L^{-1})
R^2	Correlation coefficients
$^{\circ}\text{C}$	Degree of Celsius
K_d	Distribution adsorption coefficient
m	Dry weight of the adsorbents (g)
EDX	Energy dispersive X-ray
ΔH°	Enthalpy change, (kJ mol^{-1})
ΔH_T	Enthalpy of adsorption (kJ mol^{-1})
ΔS°	Entropy change ($\text{kJ mol}^{-1} \text{K}^{-1}$)
ECH	Epichlorohydrin
C_e	Equilibrium concentration of dye in the solution (mg L^{-1})
q_e	Equilibrium dye concentration on the adsorbent (mg g^{-1})
$q_{e, exp}$	Experimental adsorption capacity of the adsorbent (mg g^{-1})
pH_f	Final pH
FTIR	Fourier transform infrared
K_F	Freundlich constants (L g^{-1})

γ	Gamma
R	Gas constant ($8.31 \text{ J mol}^{-1} \text{ K}^{-1}$),
ΔG°	Gibbs free energy change (kJ mol^{-1})
GLA	Glutaraldehyde
C_o	Initial concentration of the dye in solution (mg L^{-1})
pH_i	Initial pH
IUPAC	International Union of Pure and Applied Chemistry
k_{int}	Intra-particle diffusion rate constant ($\text{mg g}^{-1} \text{ min}^{-1/2}$)
a_L	Langmuir constant
K_L	Langmuir model constant (L mg^{-1})
k_{fd}	Liquid film diffusion constant
LCAs	Low cost adsorbents
B_t	Mathematical function represents the fraction of solute adsorbed at time, t
q_m	Maximum adsorption capacity of the adsorbents (mg g^{-1})
λ_{max}	Maximum wavelength
CsPC	PEI grafted onto Cs through CaCl_2
CsPE	PEI grafted onto Cs through ECH
CsPG	PEI grafted onto Cs through GLA
%	Percentage
k_1	PFO rate constant (min^{-1})
pH_{pzc}	pH point of zero charge
PEI	Polyethyleneimine
PFO	Pseudo-first-order
PSO	Pseudo-second-order
k_2	PSO rate constant ($\text{g mg}^{-1} \text{ min}^{-1}$)
SEM	Scanning electron microscope
R_L	Separation factor or equilibrium parameter

SSA	Solid solute adsorption
$t^{1/2}$	Square root of the contact time
B	Temkin isotherm constant
T	Temperature
t	Time
UV-Vis	Ultraviolet-Visible
V	Volume of solution (L)
v/v	Volume per volume
W	Watt
w/v	Weight per volume
XRD	X-ray diffraction

**PENYEDIAAN TERBITAN KITOSAN MELALUI MODIFIKASI
POLIETILENAIMINA UNTUK PENYINGKIRAN PEWARNA ASID
MERAH 88**

ABSTRAK

Kajian ini bertujuan untuk mencadangkan suatu kaedah alternatif untuk mensintesis penjerap yang murah, hijau dan berkesan untuk penyingkiran Asid Merah 88 (AR88) daripada larutan akueus. Kitosan telah berjaya dicangkukkan dengan polietilenaimina (PEI) melalui agen rangkai silang sama ada kalsium klorida (CaCl_2), epiklorohidrin (ECH) atau glutaraldehyd (GLA) dan masing-masing dikenali sebagai CsPC, CsPE dan CsPG. Tindak balas cangkukan dan rangkai silang dilakukan melalui sintesis satu langkah dalam sistem tertutup dengan menggunakan autoklaf keluli tahan karat, Teflon berlapis. Semasa penyediaan penjerap, kepekatan monomer dan agen rangkai silang (1 – 5 % v/v), suhu pemanasan (30 – 80 °C) serta masa pemanasan (1 – 15 h) telah dioptimumkan untuk memastikan kecekapan penjerapan yang tinggi oleh penjerap yang telah disintesis. Penjerap yang dioptimumkan telah dianalisis dengan menggunakan mikroskop electron imbasan dengan spektrometer sinar-X sebaran tenaga (SEM-EDX), spektroskopi pantulan keseluruhan dikecilkan inframerah Fourier transformasi (ATR-FTIR), pembelauan sinar-X (XRD), analisis Brunauer-Emmett-Teller (BET) dan pH takat cas sifar (pH_{pzc}). Daripada analisis-analisis ini, penjerap-penjerap tersebut menunjukkan sifat-sifat morfologi, struktur dan kimia yang unik serta mampu meningkatkan keupayaan penjerapan mereka terhadap pewarna Asid Merah 88 (AR88). Hasil dari kajian penjerapan berkelompok telah dianalisa menggunakan beberapa model isoterma iaitu Langmuir, Freundlich dan Temkin. Model Freundlich berkorelasi baik dengan data penjerapan CsPC dan CsPE yang

mencadangkan bahawa penjerapan AR88 berlaku secara multilapisan, sementara model Langmuir menggambarkan penjerapan AR88 ke atas CsPG. Model Langmuir turut menyediakan kapasiti penjerapan maksimum (q_m) bagi CsPE, CsPG and CsPC, yang masing-masing adalah 286, 435 and 1000 mg g⁻¹. Model kinetik pseudo-tertib pertama (PFO) dan pseudo-tertib kedua (PSO) telah digunakan untuk menilai data keseimbangan. Telah didapati bahawa semua process penjerapan paling baik mengikuti model kinetik PFO dengan nilai R² yang tinggi (R² ≥ 0.98) yang menunjukkan bahawa proses penjerapan adalah penjerapan fizik. Mekanisme penyebaran untuk penjerapan pewarna AR88 ke atas penjerap-penjerap telah disahkan dengan lebih lanjut menggunakan model penyerapan intra-partikel dan Boyd. Didapati bahawa kedua-dua pemindahan jisim luaran dan penyebaran intra-partikel menjejaskan langkah pengawalan kadar penjerapan. Parameter termodinamik seperti tenaga bebas Gibbs (ΔG°), entalpi (ΔH°) dan entropi (ΔS°) juga telah diperolehi dan dianalisis. Penjerapan AR88 ke atas semua penjerap-penjerap adalah eksotermik dan spontan pada suhu rendah. Berdasarkan semua penemuan di atas, CsPC, CsPE dan CsPG yang telah disintesis dalam kerja ini menunjukkan sifat penjerapan yang menggalakkan serta mampu menjadi penyerap yang menjanjikan untuk penyingkiran berkesan anion AR88 daripada larutan akueus. Di antara semua penjerap, CsPC dilihat menjadi penyerap yang terbaik dengan nilai q_m tertinggi, diikuti oleh CsPG dan CsPE.

**PREPARATION OF CHITOSAN DERIVATIVES BY
POLYETHYLENEIMINE MODIFICATION FOR THE REMOVAL OF
ACID RED 88 DYE**

ABSTRACT

This research is aimed to propose an alternative method to synthesize an inexpensive, green and effective adsorbent for the removal of Acid Red 88 (AR88) from aqueous solution. Chitosan (Cs) was successfully modified with polyethyleneimine (PEI) through a cross-linker either calcium chloride (CaCl₂), epichlorohydrin (ECH) or glutaraldehyde (GLA) and identified as CsPC, CsPE and CsPG, respectively. Grafting and cross-linking reactions were established by a one-step synthesis in a closed system by using a Teflon-lined stainless-steel autoclave. During the preparation process, polymer and cross-linker concentrations (1 – 5 % v/v), heating temperature (30 – 80 °C) as well as the heating time (1 – 15 h) were optimized to ensure high adsorption efficiency of the synthesized adsorbents. The optimized adsorbents were analyzed by using the scanning electron microscope coupled with energy dispersive X-ray spectrometer (SEM-EDX), attenuated total reflectance Fourier transform infrared (ATR-FTIR) spectroscopy, X-ray diffraction (XRD), Brunauer- Emmett-Teller (BET) and pH point of zero charge (pH_{pzc}). From these analyses, the adsorbents showed unique morphological, structural and chemical properties that improved their adsorption capabilities towards AR88 dye. The results from the batch adsorption study was analyzed by several isotherm models, namely Langmuir, Freundlich and Temkin. The Freundlich model was correlated well with the adsorption data of CsPC and CsPE, which suggested multilayer adsorption of the AR88, while Langmuir isotherm model best describes the adsorption of AR88 onto

CsPG. Langmuir model also provided the maximum adsorption capacity (q_m) for CsPE, CsPG and CsPC which are 286, 435 and 1000 mg g⁻¹, respectively. Pseudo-first-order (PFO) and pseudo-second-order (PSO) kinetic models were applied for the evaluation of the equilibrium data. It was found that the adsorption process was best fitted to the PFO kinetic model, with high R^2 value ($R^2 \geq 0.98$), indicating that the adsorption process is physisorption. The diffusion mechanism for the adsorption of AR88 dyes onto the adsorbents was further verified by the intra-particle and Boyd diffusion models. It was found that both external mass transfer and intra-particle diffusion have affected the adsorption rate controlling step. Thermodynamic parameters, Gibbs free energy (ΔG°), enthalpy (ΔH°) and entropy (ΔS°) were analyzed. The adsorption of AR88 onto the adsorbents was exothermic in nature and spontaneous at low temperature. From the above findings, CsPC, CsPE and CsPG synthesized in this work have demonstrated favorable adsorption properties and represent a promising adsorbent for the effective removal of AR88 anion from the aqueous solution. Among the adsorbents, CsPC has noted to be the best adsorbent, with the highest q_m , subsequent by CsPG and CsPE.

CHAPTER 1

INTRODUCTION

1.1 Research background

Each year, 700, 000 tons of different dyes are manufactured for their color-giving abilities and they are usually discarded into the aquatic environment once used (Katheresan *et al.*, 2018). Colors are the primary contaminant in wastewater and are highly visible even at low concentrations. They are refractory molecules that are resistant to chemical oxidation which makes them difficult to treat (Barbusi *et al.*, 2016; Crini and Badot, 2008). Figure 1.1 displays various industries responsible for the discharge of dyes into the environment (Katheresan *et al.*, 2018).

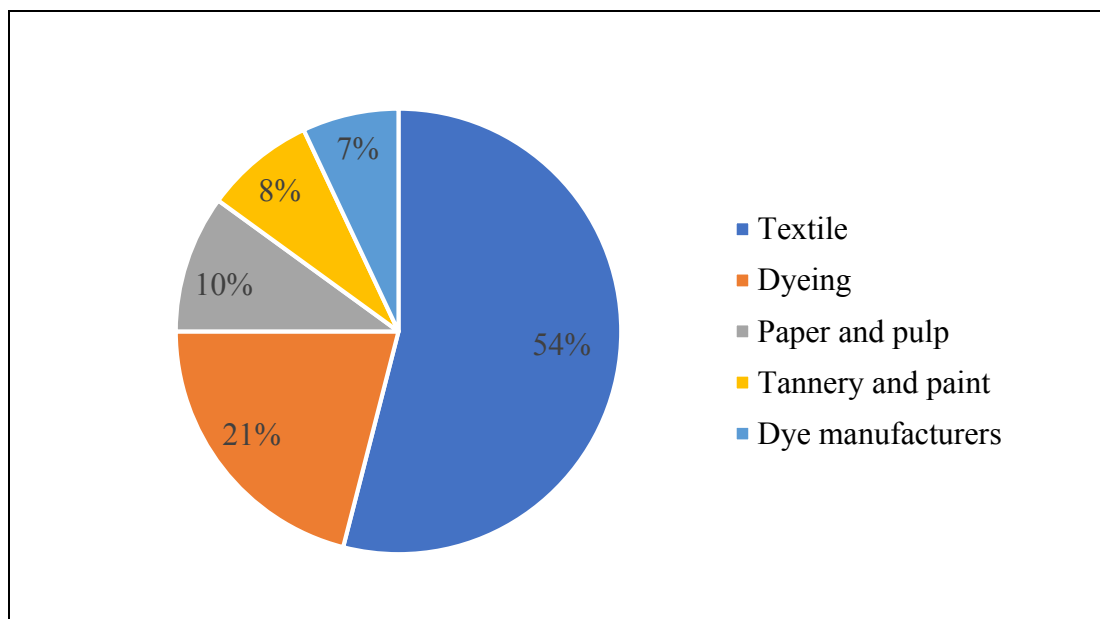


Figure 1.1: Percentages attributed by different industries on water contamination by dyes (Katheresan *et al.*, 2018).

In Malaysia, the *batik* industry is a popular inherited textile industry, especially in the East Coast of Peninsular Malaysia. Malaysia was the fifteenth largest producer of textile fiber in 2008 and ninth largest in the Asian region (Pang and Abdullah, 2013). Synthetic dye manufactured by textile, paper, paint and plastics industries becomes a

serious threat to human health, which causes skin sensitization and carcinogenicity as well as blocks the sunlight that impact the aquatic ecosystems (Gupta and Suhas, 2009). It also causes high biochemical oxygen demand, chemical oxygen demand and bad smell (Crini and Badot, 2008). There are many types of dyes and they can be classified based on their molecular structure. Chromophores and auxochromes are the important components in dyes which are responsible for producing the color and enhancing the affinity of the dye towards the fibers, respectively. Table 1.1 shows the classification of dyes generally used in textile industries.

Table 1.1: Typical dyes used in the textile industry (Salleh *et al.* 2011).

Dye class	Description
Acid	Water-soluble anionic compounds
Basic	Water-soluble, applied in weakly acidic dye baths; bright dyes
Direct	Water-soluble, anionic compounds; can be applied directly to cellulose without mordants (or metals like chromium and copper)
Disperse	Water-insoluble
Reactive	Water-soluble, anionic compounds; largest dye class
Sulfur	Organic compounds containing sulfur or sodium sulfide
Vat	Water-insoluble; oldest dyes; more chemically complex

Dyes can be generally classified into anionic, cationic and non-ionic dyes. Cationic dyes are basic dyes, while the anionic dyes are negatively charged compounds, including direct, acid and reactive dyes with the presence of azo, anthraquinone and triphenylmethane in their structure. They are usually used with silk, wool, polyamide, modified acrylic and polypropylene fibers. However, they have a dangerous effect on human beings since they are organic sulfuric acids (Salleh *et al.*, 2011).

Dyes noxiousness makes them a serious threat and cannot be discharged to the environment without being properly treated. Technologies in the removal of pollutants

can be divided into three classes which are biological, chemical and physical treatments (Crini, 2006). Biologically based methods for dye removal usually incorporate the use of living organisms like algae degradation, fungal cultures and enzyme degradation in the process. Thus, the utilization of this method with caution and engineering ethics should be upheld. However, its major disadvantage is the difficulty in predicting its reactions due to the instability growth rate of the living organism (Katheresan *et al.*, 2018).

Oxidation, ozonation, photochemical and ultraviolet irradiation are the common utilized chemical treatments. These methods are unattractive and requires specific equipment. High electrical energy is also required to power the equipment in which the chemical dye removal takes place. Besides, large consumption of chemical reagents are also reported (Katheresan *et al.*, 2018). Conventional physical dye removal methods are coagulation, flocculation, ion exchange and membrane filtration. Combination of different processes is often used to achieve the desired water quality. However, these techniques are complicated, do not provide adequate treatment, financially unfavorable and not environmentally friendly (Crini and Badot, 2008). Thus, they are not widely applied at large scale in the textile and paper industries (Crini, 2006). Despite of these methods, adsorption has triggered a broad attention in the physicochemical wastewater treatment because it has shown promising results besides of its effectiveness, economical and simplicity (Crini 2006; Gupta and Suhas 2009; Yu *et al.*, 2016).

Adsorbents that are generally used in wastewater treatment are activated carbon, alumina, silica gel and zeolites. These adsorbents are widely used due to their porous structure, large surface area (ranging from 200 – 2000 m² g⁻¹), high selectivity

and efficiency, which result in high maximum adsorption capacity, q_m (Gupta and Suhas, 2009). However, the production cost of these materials are expensive, which has attempted the researchers to search for more cost-effective adsorbents (Gupta and Suhas, 2009). Several attempts have been made on cheaper adsorbents with appreciable adsorption capacities (Crini and Badot, 2008; Gupta and Suhas, 2009) and chitosan has been seen as a potential adsorbent for various pollutants such as dyes, phenolic, herbicides, pesticides, and drugs. This is due to its physical properties, including macromolecular structure, non-toxicity, biocompatibility, and biodegradability (Kyzas and Bikiaris, 2015). Nevertheless, chitosan has low acid and thermal stability as well as inadequate mechanical strength which restrict its potentials (Zhang *et al.*, 2016) Thus, chitosan needs to be modified to further enhance its adsorption capability.

1.2 Problem statements

Grafting of a suitable monomer onto the backbone of chitosan has been reported as a promising benefit (Zhang *et al.*, 2016). However, conventional grafting initiated by free radicals brings further contamination to the final product which can be toxic to human and the environment (Konaganti *et al.*, 2010). These methods also need a longer reaction time and high temperature (Zhang *et al.*, 2014). Additionally, studies have found that chitosan tends to undergo dissolution as the amino groups will be protonated in acidic condition which limit its adsorption capabilities (Chassary *et al.*, 2005). Cross-linked chitosan has been reported to overcome this problem as well as enhancing the mechanical strength and chemical resistance of chitosan against chemicals such as alkalis and acids (Vakili *et al.*, 2014). However, low adsorption ability of the cross-linked chitosan has been reported (Liu *et al.*, 2015). Thus, it is

possible to overcome this by modifying the chitosan with another polymer. To date, the study on a one-step modification of chitosan using a cross-linker via hydrothermal technique, especially at low temperature is still lacking in literatures.

1.3 Research objectives

In order to address the aforementioned shortcomings, the objective of this study is to propose a new method for the preparation of an environmental friendly and efficient adsorbent with minimum chemical usage, short reaction time and low temperature. The specific objectives of this study are:

1. To modify the chitosan with polyethyleneimine (PEI) by hydrothermal technique by optimizing the PEI and cross-linker concentrations, temperature and heating time.
2. To physically and chemically characterize the modified chitosan by using appropriate analyses.
3. To study and evaluate the adsorption performance of the modified chitosan towards AR88 dye from aqueous solution through the adsorption isotherm, kinetic and thermodynamic models.

1.4 Scope of study

The coverage of this study consists of optimizing the operational conditions of the hydrothermal system and modified Cs such as temperature, heating time, and concentration of both PEI and the cross-linkers. The optimized CsPC, CsPE and CsPG will be characterized by using SEM-EDX, FTIR, XRD, and BET analysis to study about their physical and chemical properties. The adsorption studies on AR88 dye removal from aqueous solution for all the adsorbents will be focusing on the effect of pH (3 – 12), and initial dye concentrations ($50 - 500 \text{ mg L}^{-1}$) of the dye solution. Langmuir, Freundlich, and Temkin isotherm models, as well as the kinetic models (pseudo-first-order, pseudo-second-order, intra-particle diffusion, and Boyd model) will be applied to analyze the equilibrium and kinetics data. Besides, different thermodynamic parameters (ΔH° , ΔS° and ΔG°) of CsPC, CsPE and CsPG will be calculated in studying the effect of temperature on the adsorption of AR88 by varying the temperature from 30 – 50 °C.

CHAPTER 2

LITERATURE REVIEW

2.1 Adsorption

Adsorption is the deposition of atoms, ions or molecules from its gaseous or liquid surrounding onto the adsorbent surface (Gupta and Suhas, 2009). Adsorbate is known as the substance that accumulates on the surface, while adsorbent is the solid that provide active sites for the adsorption process to occur. The nature of the bonding (ionic, covalent or metallic) between adsorbate and the surface adsorbent depends on the properties of the species involved, which can be classified into physisorption and chemisorption (Table 2.1) (Konicki *et al.*, 2013). Physisorption happens when the adsorbed molecules are physically attracted to the solid surface of the adsorbent in nature. Van der Waals forces are responsible for this attraction, but they are not strong enough and caused reversible adsorption. As compared to chemisorption, the attraction forces between the adsorbate and adsorbent are due to covalent bonding which results in stronger bonding strength and is harder to remove from the adsorbent surface (Gupta and Suhas, 2009).

Table 2.1: Characteristics of physisorption and chemisorption (Konicki *et al.*, 2013).

Characteristics	Physisorption	Chemisorption
Bonding between adsorbent and adsorbate	Van der walls or hydrogen bonding	Covalent bonding
Activation energy, E_a (kJ mol ⁻¹)	5 – 40	40 – 800
The Gibbs free energy change, ΔG° (kJ mol ⁻¹)	-20 – 0	80 – 400
The enthalpy change, ΔH° (kJ mol ⁻¹)	4 – 40	40 – 800

It is also reported that the activation energy of physical adsorption is between 5 to 40 kJ mol⁻¹ and the Gibbs free energy change is between -20 to 0 kJ mol⁻¹. While, the activation energy for chemical adsorption ranges from 40 to 800 kJ mol⁻¹ and Gibbs free energy change between 80 to 400 kJ mol⁻¹ (Konicki *et al.*, 2013). In addition, the adsorption process involving physisorption has an enthalpy value smaller than that of chemisorption. Typically, the enthalpy change of physisorption ranges between 4 to 40 kJ mol⁻¹ while the enthalpy change of chemisorption ranges from 40 to 800 kJ mol⁻¹. For better understanding, a series of adsorption experiments in a batch system is usually conducted to evaluate the adsorption data and study its phenomena at the solid/liquid interface (Crini and Badot, 2008).

2.2 Adsorption isotherm

Adsorption isotherm enables the interpretation of the equilibrium distribution of dye molecules between the solid adsorbent and the liquid phase at a given temperature. Equilibrium studies give the capacity of the adsorbent and describe the suitable adsorption isotherm by constants which express the surface properties and information about the structure of the adsorbed layer (Foo and Hameed, 2010). Surface area and pore diameter govern the type of adsorption isotherm. Pore sizes are generally categorized into three types according to their relative diameter size. Macropores have a diameter of more than 50 nm, mesopores ranging between 2 and 50 nm, while micropores have the smallest pore diameter of less than 2 nm (IUPAC, 1972).

Adsorbates adsorbed on the solid surface can be in three different states of matter which are gasses, liquids and solids. However, solid solute adsorption (SSA) is more complex compared to vapor or gas adsorption (VPA) and composite liquid adsorption (CLA). This is because it involved different types of interaction, such as

adsorbent-adsorbate, adsorbent-adsorbent, and adsorbate-adsorbate (Giles *et al.*, 1974). SSA isotherms can be described in four classes which are sigmoidal (S), Langmuir (L), high affinity (H) and constant partition (C) and further into several subgroups of 1, 2, 3, 4 and max as shown in Figure 2.1.

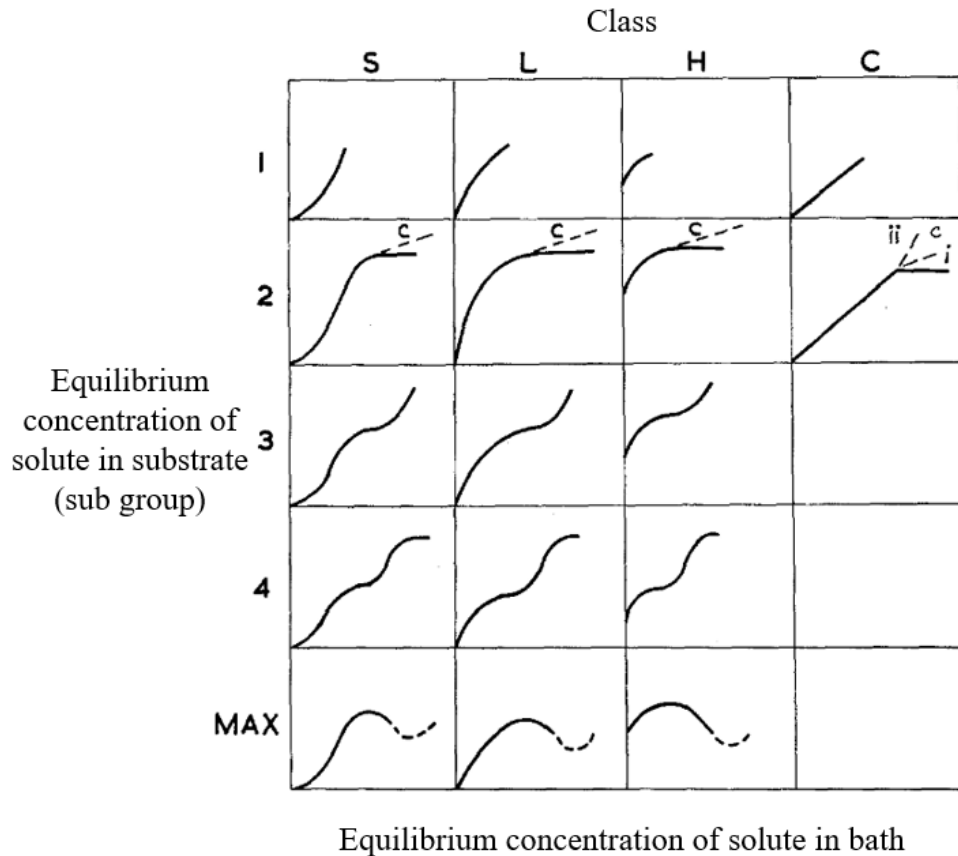


Figure 2.1: System of isotherm classification for solid solute adsorption (SSA) (Giles *et al.*, 1974).

The classification of isotherm shapes gives the necessary details on the adsorption mechanism and therefore, can be used to diagnose the nature of the adsorption. For instance, the S-type isotherm describes that the interaction of adsorbate-adsorbate is stronger compared to adsorbate-adsorbent interaction (Giles *et al.*, 1974). In this case, the activation energy needed to remove adsorbate from adsorbent is concentration dependent. On the other hand, the adsorbate-adsorbent

interactions are very weak while the adsorbent-adsorbate interaction is relatively strong for L and H isotherms (Giles *et al.*, 1974). The C-type isotherm represents a constant relative affinity of solute for the adsorbent. Apparently, the C-type isotherm is usually observed at a low range of adsorption (Giles *et al.*, 1974).

Based on the shape of the isotherms at higher concentrations, each class is further categorized into subgroups of 1, 2, 3, 4 and max. The curves in subgroup 1 represent system in which the adsorbate monolayer has not been completed and in the subgroups 2, the completion of the first monolayer can be identified (Giles *et al.*, 1974). The subsequent rise of subgroup 3 and 4 represents the development of a second layer after the completion of the first monolayer where the adsorbate is attracted by a layer of its own molecule (Giles *et al.*, 1974). The attractive forces are generally weaker than those forces generated in the first layer. This condition explained the S-shaped appeared as the isotherm changes from subgroup 2 to 3 or 4. L2 and H2 are the common curves for the adsorption of ionic adsorbates as shown in Figure 2.1. The second layer is reluctant to form because of the columbic repulsive force in the first layer (Giles *et al.*, 1974). The adsorption process reaches equilibrium when the rate of adsorption and desorption are equal. The Langmuir, Freundlich and Temkin models are the well-known adsorption isotherm model for describing the adsorption process (Crini and Badot, 2008).

2.2.1 Langmuir isotherm model

This model was proposed by Langmuir (1918) to explain the adsorption of hydrogen gas on the palladium surface. He suggested that the nature of the material was a homogeneous surface where the adsorption sites on the material have equal energy for adsorption regardless of the distance between the sites (Chen *et al.*, 2016).

It is also assumed that the adsorbed dye molecules do not interact with one another or migrate over the surface after adsorption (Foo and Hameed, 2010). After the monolayer surface becomes saturated, no further adsorption can happen at the site and therefore reached the maximum adsorption (Langmuir, 1918). The equation is given as below (Langmuir, 1918):

$$q_e = \frac{K_L q_m C_e}{1 + K_L C_e} \quad (2.1)$$

where q_e is the equilibrium dye concentration (mg g^{-1}) on the adsorbent, q_m is the maximum adsorption capacity of the adsorbents (mg g^{-1}), K_L is the Langmuir model constant related to adsorption energy (L mg^{-1}) and C_e is the equilibrium concentration of dye (mg L^{-1}) in the solution.

Equation (2.1) can be expressed in a linear form which is defined by Equation (1.2):

$$\frac{C_e}{q_e} = \frac{1}{q_m K_L} + \frac{C_e}{q_m} \quad (2.2)$$

Another Langmuir constant can also be written as a_L which describes the binding strength between adsorbent and adsorbate using the equation below (Kabir *et al.*, 2014):

$$a_L = \frac{K_L}{q_m} \quad (2.3)$$

The behavior of the adsorption process can be expressed in terms of the dimensionless constant separation factor or equilibrium parameter, R_L (Dehghani *et al.*, 2017) which is defined by:

$$R_L = \frac{1}{1 + K_L C_o} \quad (2.4)$$

where C_o is the initial concentration of the dye in solution (mg L^{-1}). The value of R_L indicates the type of isotherm to be irreversible ($R_L = 0$), favorable ($0 < R_L < 1$) or unfavorable ($R_L > 1$).

2.2.2 Freundlich isotherm model

The Freundlich isotherm model is used to describe the non-ideal and reversible adsorption. This model can be employed to multilayer adsorption and assumed that the heat of adsorption for every sorptive site is not uniform (Foo and Hameed, 2010). The expression of the model is presented below (Freundlich, 1906):

$$q_e = K_F C_e^{\left(\frac{1}{n}\right)} \quad (2.5)$$

and can be linearized as below:

$$\log q_e = \log K_F + \frac{1}{n \log C_e} \quad (2.6)$$

where K_F and n are the Freundlich constants (L g^{-1}), and adsorption intensity of the adsorption process, respectively.

The Freundlich constant, n represents the parameter characterizing quasi-Gaussian energetic heterogeneity of the adsorption surface. It gives an indication on the favorability of adsorption. The value of n in the range 1 – 10 represent good while less than 1 is a poor adsorption characteristic (Deng *et al.*, 2011).

2.2.3 Temkin isotherm model

The Temkin isotherm deals with the interaction between adsorbent and adsorbate and the heat of adsorption of all molecules in the layer would decrease exponentially, ignoring very low and high concentrations (Foo and Hameed, 2010). The derivation of this equation is characterized by a uniform distribution of binding

energy (Puttamat and Pavarajarn, 2016). The nonlinear form is described by Equation (2.7) (Temkin and Pyzhev, 1940):

$$q_e = B \ln(AC_e) \quad (2.7)$$

while the linearized Temkin isotherm is written as:

$$q_e = B \ln A + B \ln C_e \quad (2.8)$$

The term, $B = RT/\Delta H_T$, is Temkin isotherm constant which is associated with adsorbent-adsorbate interaction, ΔH_T corresponds to the enthalpy of adsorption (kJ mol^{-1}), R is the gas constant ($8.31 \text{ J mol}^{-1} \text{ K}^{-1}$), T is the absolute temperature (K), and A is the binding constant at equilibrium which corresponds to the maximum binding energy (L g^{-1}).

2.3 Adsorption kinetics

The existence of unbalanced or remaining forces at the surface of liquid and solid phase arises the process of adsorption (Nakhjiri *et al.*, 2018). These unbalanced remaining forces tend to attract and retain the molecular species in contact with the surface. When adsorption is concerned, kinetic aspects should be involved to know more details about its performance and mechanism. Adsorption kinetics is the base to determine the performance of the adsorption process and can be categorized into adsorption reaction and adsorption diffusion models (Qiu *et al.*, 2009). Several adsorption reaction models originated from chemical kinetics that based on the whole process of adsorption have been developed which are pseudo-first-order (PFO), and pseudo-second-order (PSO). They are the most widely used kinetic models to describe the adsorption process (Qiu *et al.*, 2009). A separate set of adsorption experiments at different time interval and constant temperature is carried out to study the kinetics of the adsorption process. The kinetics also can be studied at a different temperature. This

information is useful for further applications of the system design in the treatment of natural water and waste effluents.

2.3.1 Pseudo-first-order model

The pseudo-first-order (PFO) kinetic model was first proposed by Lagergren at the end of 19th century to describe the kinetic process of liquid-solid phase adsorption of oxalic acid and malonic acid onto charcoal (Qiu *et al.*, 2009). The rate equation was the earliest equation for sorption in a liquid system based on solid capacity and presented as follows (Lagergren, 1898):

$$\frac{dq_t}{dt} = k_1(q_e - q_t) \quad (2.9)$$

This equation can be rearranged into the linear equation as follows:

$$\log(q_e - q_t) = \log q_e - \frac{k_1}{2.303}t \quad (2.10)$$

where q_e (mg g⁻¹) and q_t (mg g⁻¹) are the amounts of dye adsorbed on the adsorbent at equilibrium and at time t , respectively; and k_1 (min⁻¹) is the PFO rate constant.

2.3.2 Pseudo-second-order model

The pseudo-second-order (PSO) kinetic model was introduced in the middle of the 80's and received more attention when Ho and McKay (1998) discussed the adsorption kinetic of divalent metal ions onto peat which favored PSO than PFO. The applicability of the PSO model suggested that chemisorption is the rate-limiting step that controls the adsorption process involving the valence force through sharing or the exchange of electrons between the adsorbent and adsorbate (Crini and Badot, 2008; Qiu *et al.*, 2009). The PSO rate equation is expressed as given below (Ho and McKay, 1998):

$$\frac{dq_t}{dt} = k_2(q_e - q_t)^2 \quad (2.11)$$

Equation (2.11) can be rearranged into a linear form and is given by:

$$\frac{t}{q_t} = \frac{1}{k_2 q_e^2} + \frac{t}{q_e} \quad (2.12)$$

where q_e and q_t are the sorption capacities at equilibrium and at time, t (min) respectively, while k_2 is the PSO rate constant ($\text{g mg}^{-1} \text{min}^{-1}$).

2.4 Diffusion-controlled sorption mechanism

Adsorption reaction model and adsorption diffusion model are different in nature. Compared to the adsorption reaction model which based on the whole process of adsorption, adsorption diffusion model constructed based on three consecutive steps (Qiu *et al.*, 2009):

- i. Diffusion of adsorbates across the liquid surrounding the adsorbent surface (external or film diffusion),
- ii. Diffusion of adsorbates into the pores (intra-particle diffusion) and,
- iii. Adsorption and desorption between the adsorbate and active sites (mass action)

For physical adsorption, mass action is a rapid process and can be negligible for kinetic study. Thus, the rate-determining step of adsorption is controlled by intra-particle and/or film diffusion. The adsorption diffusion model can be used to describe these processes (Qiu *et al.*, 2009).

The intra-particle diffusion is elucidated by Weber and Morris (1963). They proposed that in many adsorption cases, adsorbates uptake varies almost proportionally with the square root of the contact time, $t^{1/2}$ rather than the contact time, t . They are predicting that if the rate-limiting step is intra-particle diffusion, the plot of

adsorbates uptake against $t^{1/2}$ yield a straight line passing through the origin. Good linearization of the data is observed in the initial phase of the reaction in accordance with expected behavior if intra-particle diffusion is the rate-limiting step (Ofomaja, 2010). The widely used intra-particle diffusion equation for the biosorption system is given by (Weber and Morris, 1963):

$$q_t = k_{int}t^{1/2} + C \quad (2.13)$$

where k_{int} is the intra-particle diffusion rate constant ($\text{mg g}^{-1} \text{min}^{-1/2}$) and the intercept C is the boundary layer thickness (mg g^{-1}) obtained from the extrapolation of the linear portion of the plot of q_t versus $t^{1/2}$.

The film diffusion equation was presented by Boyd *et al.* (1947). The Boyd plot predicts the actual slow step involved in the adsorption process (Nethaji *et al.*, 2013). The Boyd kinetic expression is given by (Boyd *et al.*, 1947):

$$B_t = -0.4977 - \ln\left(1 - \frac{q_t}{q_e}\right) \quad (2.14)$$

where B_t is the mathematical function representing the fraction of solute adsorbed at time, t (min) and k_{fd} is the liquid film diffusion constant determined from the gradient of the linear plot between $\ln(1 - q_t/q_e)$ and t .

2.5 Thermodynamics

The effect of different temperature on the adsorption process can be studied by determining the thermodynamic parameters which are the changes in standard enthalpy (ΔH°), standard entropy (ΔS°) and standard free energy (ΔG°). The values of ΔH° , ΔS° and ΔG° are calculated using the following equations (Gibbs, 1873):

$$\Delta G^\circ = -RT \ln K_d \quad (2.15)$$

$$\Delta G^\circ = \Delta H^\circ - T\Delta S^\circ \quad (2.16)$$

where R ($8.314 \text{ J mol}^{-1} \text{ K}^{-1}$) is the gas constant and T (K) is the absolute solution temperature. The distribution adsorption coefficient, K_d is calculated from the following equation (Kamari *et al.*, 2009):

$$K_d = \frac{C_{Ad}}{C_e} \quad (2.17)$$

where C_{Ad} is the concentrations of the adsorbate adsorbed on solid at equilibrium (mg L^{-1}), and C_e is the equilibrium concentration of the adsorbate in the solution (mg L^{-1}). From the Equation (2.15) and (2.16), the van't Hoff equation can be obtained as (Kamari *et al.*, 2009):

$$\ln K_d = \frac{\Delta S^\circ}{R} - \frac{\Delta H^\circ}{RT} \quad (2.18)$$

The plot of $\ln K_d$ versus $1/T$ gives a straight line with a slope of ΔH° (kJ mol^{-1}) and an intercept of ΔS° ($\text{kJ mol}^{-1} \text{ K}^{-1}$), while the value of K_d used in determination of ΔG° (kJ mol^{-1}).

2.6 Low cost adsorbents (LCAs)

Low-cost adsorbents (LCAs) have been an alternative to replace commercial activated carbon (Crini, 2006). They are usually derived from wastes or by-products from either agricultural or industrial wastes (bagasse pith, maize cob, rice husk, coconut shell, metal hydroxide sludge) because of their high availability (Crini, 2006; Gupta and Suhas, 2009). LCAs can also be manufactured from natural resources and or with minor treatments such as wood, coal, peat, chitin, biomass, cotton, clays, starch, and others (Crini, 2006; Gupta and Suhas, 2009). Their adsorption capability towards dyes have been reported in various studies such as removal of Methylene Blue by peat (Neves *et al.* 2010), Safranin-O by Loy Yang high sodium (LYNA) brown coal and Acid Red18 by poplar woods (Heibati *et al.* 2015). Compared to all these adsorbents,

manufacturing of chitosan from naturally occurring chitin has become an interesting topic these days. In recent studies, chitosan has been reported to have outstanding removal properties in removing Reactive Black 5 (Chatterjee *et al.*, 2011), Amido Black 10B (Liu *et al.*, 2015) and Acid Red 37 (Kamari *et al.*, 2009) from aqueous solution with high adsorption capacity of 709.27, 323.60, and 357.14 mg g⁻¹, respectively. From these examples, chitosan is a promising adsorbent in countering the disadvantages of commercial adsorbents, such as activated carbon. Nevertheless, some modifications are needed to enhance their adsorption capabilities depending on the type of target pollutants.

2.7 Chitosan

2.7.1 Production of chitosan

Chitosan is produced from chitin (Figure 2.2), a low-cost material and known as the second most abundant nitrogenous polysaccharide in nature after cellulose (Zohuriaan-mehr, 2005). It is known as biosorbent because it is a biological material which is able to form chelating and complexing sorbents in order to remove dyes from aqueous solutions (Crini, 2006).

It can be found in the exoskeleton of marine crustaceans predominantly due to the large availability of wastes from food processing industry. It is extracted from the exoskeletons of shrimps and crabs by acid treatment to dissolve the calcium carbonate in their shells followed by alkaline extraction to dissolve the proteins (Zohuriaan-mehr, 2005). Finally, it undergoes a decolorization step to remove residual pigments before a colorless product is obtained.

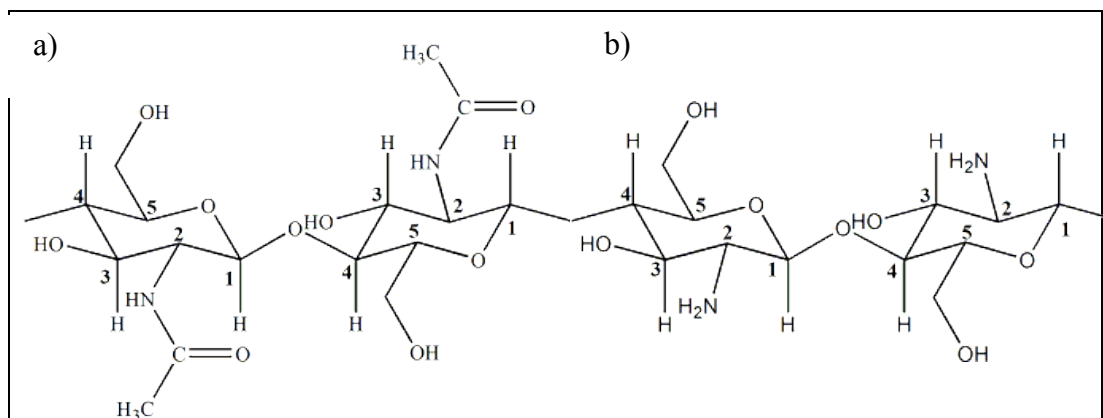


Figure 2.2: Structure of (a) chitin and (b) partially deacetylate chitosan (Zohuriaan-mehr, 2005).

Chitin is structurally alike cellulose with a linear homopolymer composed of $\beta(1\rightarrow4)$ -linked 2-acetamido-2-deoxy- β -D-glucose (*N*-acetylglucosamine), but it has acetamide groups at the C2 positions instead of the hydroxyl groups (Crini and Badot, 2008). The presence of this group is highly advantageous since it provides particular adsorption functions and reactions for modification (Crini and Badot, 2008). However, the slow biodegradation rate and insolubility of chitin, accompanied with various problems such as weak extent of reaction, difficulty in selective substitution and structural ambiguity of the products have become an issue in the food processing industry which limit its uses (Zohuriaan-mehr 2005).

Chitin undergoes alkaline deacetylation using sodium hydroxide to form an acid-soluble product called chitosan or its scientific name given as α -(1 \rightarrow 4)linked 2-amino-2-deoxy- β -D-glucose (Vakili *et al.*, 2014). Chitin and chitosan names literally correlate to the presence of acetyl content (Zohuriaan-mehr, 2005). Chitosan generally has acetyl content of less than 25% and there is a different degree of deacetylation commercially available (Crini and Badot, 2008).

2.7.2 Properties of chitosan

Chitosan is popular among the other polysaccharides because of its chemical structure. It is composed of two reactive functional groups which are amino and hydroxyl groups. These functional groups allow chemical modifications on chitosan to enhance its particular purpose with fewer complications (Crini and Badot, 2008). Other properties of this biopolymer have been summarized in Table 2.2. Chitosan is a non-toxic, linear, heterogeneous, cationic and a biodegradable polyamine with high molecular weight. It has a rigid D-glucosamine structure, high crystallinity and hydrophilicity. It forms salts with organic and inorganic acids. Its bioactivities include antimicrobial (fungi, bacteria, viruses), antiulcer and antitumor properties, blood anticoagulants, hypolipidemic activity and bioadhesivity (Crini and Badot, 2008). It is insoluble in water, alkaline solutions and organic solvents because of the hydrogen bonds between its molecules (Vakili *et al.*, 2014).

Other appealing intrinsic properties were also reported in a review by Crini and Badot (2008) such as biodegradability, biocompatibility, film-forming ability, bioadhesivity, polyfunctionality, hydrophilicity and adsorption properties. The cationic nature of chitosan played an important role for most of these properties which lead to the concession of this polyamine as a promising raw material for adsorption purposes (Crini and Badot, 2008). Reactive amino groups are responsible for chemical activation, cross-linking and chelation of metal cations in the near-neutral pH range (Chassary *et al.*, 2005). These cationic properties have made the biopolymer an efficient adsorbent for metal and dye anions through electrostatic attraction (Chassary *et al.*, 2005).

Despite of all the advantages, there are also some unfavorable circumstances of its practical applications in wastewater treatment. Being a biodegradable biopolymer make chitosan an environmentally friendly product, but this is inconvenience to the industry for a long term application (Crini and Badot, 2008). Another important criterion to be considered concerns the variability and heterogeneity of the polymer. The distribution of the acetyl groups along the backbone is hard to control which makes it difficult to get reproducible initial polymers. Besides, the adsorption properties depend on the quality of commercial chitin and its sources (Crini and Badot, 2008).

Although the presence of amino groups is seen to benefit adsorption purpose through their protonation, but it leads to total or partial dissolution of the chitosan in acidic solutions (except in sulfuric acid). This character makes the chitosan less stable and also sensitive to pH (Chassary *et al.*, 2005). Most of the amine amino group protonated at pH below than 5.5 (Chassary *et al.*, 2005; Yang *et al.*, 2016). Thus, it is necessary to reinforce its chemical stability and one of the methods is by a chemical cross-linking. Glutaraldehyde is one of the famous cross-linkers that is widely used to solve this problem. Its aldehyde functions will react with amine groups of chitosan to form imine functions that lead to the insolubility of the polymer even at low pH (Chassary *et al.*, 2005). Another problem is with its physicochemical characteristics, in particular, low surface area, porosity and mechanical strength. These limit the adsorption performance of this polyamine (Crini and Badot, 2008; Vakili *et al.*, 2014).

2.7.3 Applications of chitosan

Studies on chitosan and its derivatives have grown exponentially due to its non-toxicity, biodegradability and biocompatibility which exhibited high potential in different products and applications. Table 2.2 shows the chitosan properties with various purposes in wastewater treatment.

Table 2.2: Chitosan properties in relation to the water and waste treatment applications (Renault *et al.*, 2009).

Chitosan properties	Potential applications
Non-toxic Biodegradable	Flocculant to clarify water Reduction of turbidity in food processing effluents
Renewable resource	Coagulation of suspended solids, mineral and organic suspensions
Ecologically acceptable polymer (eliminating synthetic polymers, environmentally friendly)	Flocculation of bacterial suspensions
Efficient against bacteria, viruses, fungi	Interactions with negatively charged molecules
Formation of salts with organic and inorganic acids	Recovery of valuable products (proteins, etc.)
Ability to form hydrogen bonds intermolecularly	Chelation of metal ions
Ability to encapsulate	Removal of dye molecules by adsorption processes
Removal of pollutant's with outstanding pollutant-binding capacities	Reduction of odors, sludge treatment, filtration and separation, polymer assisted ultrafiltration

Chitosan is sometimes modified to maximize its solubility, antimicrobial activity and its ability to interact with other substances (Anitha *et al.*, 2012) for applications ranging from pharmaceutical, cosmetics, plant protection and water treatment (Dutta *et al.*, 2004). This amino-biopolymer has received great attention as

useful coagulants, flocculants and chelating agents in water treatment processes for the removal of various contaminants, including heavy metals (Wan Ngah *et al.*, 2004), pesticide (Yan *et al.*, 2013), phenols (Jawad and Nawi, 2012) and dyes (Sadeghi-Kiakhani *et al.*, 2013).

2.8 Modification of chitosan

2.8.1 Physical modification

Chitosan is physically modified in different forms such as flakes, powders, beads and films on the consideration of the favorable properties and applications of the derivatives (Chassary *et al.*, 2005). Chitosan derivatives in dispersed forms like bead, flakes and powders provide a high active surface area and exhibit good adsorption performance for numerous dyes (Crini and Badot, 2008; Salehi *et al.*, 2016). This is supported with the finding by Subramani and Thinakaran (2016) in synthesizing chitosan powder from prawn shell and its capability to remove Reactive Red from aqueous solution with high adsorption capacities of 1250 mg g⁻¹.

The transformation of raw chitosan flakes and powder into beads has also been reported to improve the adsorption performance by enhancing the porosity and surface area (Vakili *et al.*, 2014). Gel beads formation under alkaline solution allows an expansion of the polymer network (Azlan *et al.*, 2009). The rigidity of the polymer is due to the hydrogen bonding between the chitosan chains. These bonds are favored to be destructed and caused the expansion of the polymers network, which enhanced the diffusion of dyes from aqueous solutions to the internal sorption sites and reduced the crystalline state of chitosan (Guibal and Tobin, 1998). Besides, a comparison of specific surface area between the chitosan flakes and beads shows a large increase in

the surface area which indicates that the expansion may represent the most significant cause for the enhancement of sorption properties (Guibal and Tobin, 1998).

Another physical modification includes a film or membrane form which is made by casting the chitosan solution mixed with alkali into a flat surface to evaporate the solvent (Vakili *et al.*, 2014). This is an alternative to facilitate the separation phase after the adsorption process. Besides, films are an attractive way in the removal of pollutants from aqueous solutions due to its good mechanical properties. However, it suffers from some drawbacks such as vulnerability in acidic media, poor thermal resistance, low surface area and, porosity as well as weak mechanical strength which encourage researchers to consider modifying this material with other chemicals into desirable products (Chassary *et al.*, 2005; Vakili *et al.*, 2014).

2.8.2 Chemical modification

The basic structure of chitosan is not changed after chemical modification but brings new derivatives with improved properties for special applications in various areas. The mechanical properties, chemical stability and adsorption ability of raw chitosan can be enhanced by chemical modifications. It also decreases the biochemical and microbiological degradation of chitosan (Vakili *et al.*, 2014). Presence of reactive functional groups, an amino as well as both primary and secondary hydroxyl groups at the C2, C3 and C6 positions (refer Figure 1.3(b)), respectively, on chitosan allow modifications to take place, especially on the C2 position with few complications (Chassary *et al.*, 2005; Crini and Badot, 2008). The derivation is an appropriate modification to manipulate properties of chitosan and yield various practical substances for different potential applications (Vakili *et al.*, 2014). Cross-linking and graft copolymerization are expected to be the most promising approaches to a wide